



Original Paper

Influence of glycol ether additive with low molecular weight on the interactions between CO₂ and oil: Applications for enhanced shale oil recovery



Huan Zhang^{a, b}, Hou-Jian Gong^{a, b, *}, Wei Lv^{a, b}, Ji-Wei Lv^{a, b}, Miao-Miao Gao^{a, b}, Shang-Lin Wu^{a, b}, Hai Sun^{a, b}, Long Xu^{a, b}, Ming-Zhe Dong^c

^a Key Laboratory of Unconventional Oil & Gas Development (China University of Petroleum (East China)), Ministry of Education, Qingdao, 266580, Shandong, China

^b School of Petroleum Engineering, China University of Petroleum (East China), Qingdao, 266580, Shandong, China

^c Department of Chemical and Petroleum Engineering, University of Calgary, Calgary, Alberta, T2N 1N4, Canada

ARTICLE INFO

Article history:

Received 6 November 2023

Received in revised form

2 June 2024

Accepted 5 June 2024

Available online 7 June 2024

Edited by Yan-Hua Sun

Keywords:

Glycol ether additive

Cloud point pressure

Interfacial tension

Extraction

Expansion

ABSTRACT

The high-efficient development of shale oil is one of the urgent problems in the petroleum industry. The technology of CO₂ enhanced oil recovery (EOR) has shown significant effects in developing shale oil. The effects of several glycol ether additives with low molecular weight on the interactions between CO₂ and oil were investigated here. The solubility of glycol ether additive in CO₂ was firstly characterized. Then, the effects of glycol ether additives on the interfacial tension (IFT) between CO₂ and hexadecane and the volume expansion and extraction performance between CO₂ and hexadecane under different pressures was investigated. The experimental results show that diethylene glycol dimethyl ether (DEG), triethylene glycol dimethyl ether (TEG), and tetraethylene glycol dimethyl ether (TTEG) all have low cloud point pressure and high affinity with CO₂. Under the same mass fraction, DGE has the best effect to reduce the IFT between hexadecane and CO₂ by more than 30.0%, while an overall reduction of 20.0%–30.0% for TEG and 10.0%–20.0% for TTEG. A new method to measure the extraction and expansion rates has been established and can calculate the swelling factor accurately. After adding 1.0% DEG, the expansion and extraction amounts of CO₂ for hexadecane are respectively increased to 1.75 times and 2.25 times. The results show that glycol ether additives assisted CO₂ have potential application for EOR. This study can provide theoretical guidance for the optimization of CO₂ composite systems for oil displacement.

© 2024 The Authors. Publishing services by Elsevier B.V. on behalf of KeAi Communications Co. Ltd. This is an open access article under the CC BY-NC-ND license (<http://creativecommons.org/licenses/by-nc-nd/4.0/>).

1. Introduction

In recent years, the exploration and development of unconventional oil and gas has gradually increased worldwide (Taheri-Shakib and Kantzas, 2021). Shale oil reserves are enormous in the world. According to preliminary calculations, shale oil reserves are about 11 trillion to 13 trillion tons, far exceeding conventional oil reserves (Jia et al., 2019; Yang and Jin, 2019). Shale reservoirs have complex reservoir and fluid characteristics, complex pore structures, diverse mineral composition, rich organic matter, and diverse

crude oil occurrence states, leading to more incredible difficulty in development and low recovery (Fu et al., 2020; Jiang et al., 2016; Xu et al., 2022).

Horizontal well-mining technology and multistage hydraulic fracturing technology are the primary means to develop shale oil reserves (Feng et al., 2020), and supplementing formation energy is key to achieve sustainable and efficient development of shale oil after hydraulic fracturing (Feng et al., 2020; Xu et al., 2022; Yu et al., 2015). Due to the low permeability of shale oil reservoirs, water flooding cannot be effectively applied in shale oil reservoirs, mainly because the clay in shale reservoirs expands with water, strong heterogeneity results in a low sweep coefficient of water flooding, and low permeability results in poor water flooding injection ability, while gas injection development can effectively avoid the above issues (Ozowe et al., 2020).

* Corresponding author. Key Laboratory of Unconventional Oil & Gas Development (China University of Petroleum (East China)), Ministry of Education, Qingdao, 266580, Shandong, China.

E-mail address: gonghoujian@upc.edu.cn (H.-J. Gong).

In the petroleum industry, CO₂-EOR technology is considered the most economically viable technology for carbon capture, usage, and storage (Zhang K. et al., 2020). Furthermore, the CO₂-EOR technology shows remarkable effects when applied to low-porosity and low-permeability oil reservoirs (Song et al., 2022; Tang et al., 2023).

The injection of CO₂ can reduce oil viscosity, extract crude oil, and promote oil swelling (Lang et al., 2021; Liu et al., 2022). Due to the high affinity between CO₂ and organic matter, the crude oil in the adsorption miscible state in shale organic matter can be effectively used (Dong et al., 2022). Survey results show that the recovery rate of CO₂ miscible flooding is higher than that of immiscible flooding, meaning more crude oil can be extracted under the same conditions (Kumar et al., 2022; Zhang et al., 2018). Factors affecting miscible flooding include oil composition, gas injection type, reservoir temperature, and pressure (Dong et al., 2022; Yang et al., 2021). However, due to the limitations of current technology and the complexity of the reservoir environment, achieving CO₂ miscible flooding presents challenges (Almobarak et al., 2021; Janna and Le-Hussain, 2020). How to effectively reduce the IFT between CO₂ and oil and promote the miscibility of CO₂ with oil is of great significance for strengthening the interaction mechanism between CO₂ and oil and improving CO₂-EOR technology (Sheng, 2015; Zou et al., 2015).

The design and selection of effective additives can effectively promote the miscibility of CO₂ and crude oil. Associated gas is often injected into the reservoir to promote the miscibility of CO₂ and crude oil (Choubineh et al., 2019; Ozowe et al., 2020), but the high cost and the diversity of reservoirs limit the widespread application of this technology. Low-carbon alcohols can effectively reduce the miscible pressure of CO₂-crude oil, but the application costs are relatively high (Moradi et al., 2014; Saira et al., 2020, 2021). The addition of surfactants have significant effects in reducing the IFT between oil and water, emulsifying crude oil, and altering the wettability of rocks (Kharazi et al., 2023a, 2023b; Li et al., 2012; Saïen et al., 2023). The addition of ethanol can promote the dissolution of surfactants in CO₂, and there is a synergistic enhancement mechanism in reducing the IFT between CO₂ and crude oil (Zhang C. et al., 2020). Non-ionic surfactants typically have high solubility in CO₂ and oil.

As early as 1990, Consan and Smith (1990) evaluated the solubility of over 130 surfactants in CO₂ and found that surfactants containing fluorine and silicon-based groups had higher solubility in CO₂. Fluorinated and silicone surfactants are relatively more toxic, whereas hydrocarbon surfactants are more favored due to their environmental friendliness and lower cost (Beckman, 2004). It has been confirmed by a large number of experiments that hydrocarbon containing polyoxypropylene groups, polyoxyethylene groups, ester groups, and carbonyl groups have high solubility in CO₂ due to the interaction of Lewis acid-Lewis base and hydrogen bond (Consan and Smith, 1990; Kauffman, 2001; Kazarian et al., 1996; Lv et al., 2020; Tsukahara et al., 2004), and has a significant improvement effect on enhancing oil recovery (Luo et al., 2018; Lv et al., 2024). This provides valuable experience for selecting suitable CO₂+additive composite systems.

Additive-assisted CO₂ injection for shale oil development requires considering the solubility in CO₂ and the geological characteristics of the reservoir. For additives with larger molecular weights, it is easy to cause pore blockage in low-porosity and low-permeability shale reservoirs, and the adsorption effect of organic matter kerogen is more significant. In recent years, dimethyl ether (DME) has been used to eliminate liquid blockage in unconventional gas/condensate reservoirs (Ganjdanesh et al., 2016; Sayed and Al-Muntasheri, 2014), and the pilot test of DME-assisted CO₂ injection in underground oil recovery in the Alabama oilfield has

been successful conducted. Kong et al. (2021) compared DME and traditional additives such as propane and *n*-butane and found that DME-assisted CO₂ injection into the reservoir significantly reduced crude oil viscosity and the IFT between CO₂ and oil.

Although DME has a good effect on CO₂ injection in the oilfield, DME has specific toxicity and is flammable and explosive. Looking for a CO₂ composite system with green, pollution-free, and excellent performance has become importance to the CO₂ application in shale oil production. Based on this, DEG, TEG, and TTEG, which contain glycol group and have low molecular weight, are selected in this paper. The solubility of the three polyethylene glycol dimethyl ether additives in CO₂ was evaluated by the cloud point pressure measurement in the CO₂ phase equilibrium device. The ability to reduce the IFT between CO₂ and oil and the effect of polyethylene glycol dimethyl ether additives on CO₂ extraction and expansion performance were investigated and quantitatively analyzed. The goal of this study is to provide theoretical guidance for selecting CO₂ composite systems in oilfields.

2. Experimental method

2.1. Experimental chemicals and devices

The CO₂ used in the experiment was provided by Qingdao Tianyuan Industrial Gas Co., LTD. (purity 99.8%). DEG, TEG, and TTEG were supplied by Shanghai McLean Biochemical Technology Co., LTD. (purity 99.5%). Hexadecane provided by Sinopharm Chemical Reagent Co., LTD. was used as the simulated shale oil to ensure the experiment's repeatability. Ethanol with a purity of 99.5% was also supplied by Sinopharm Chemical Reagent Co., LTD.

The high-pressure visual cell used in the experiment was produced by Jiangsu Hai'an Scientific Research Instrument Co., LTD., with a pressure of up to 30.0 MPa. The IFT/high-pressure drop shape analyzer DSA100HP40 was provided by Kruss Company, Germany.

2.2. Experimental principle and procedure

2.2.1. Measurement of the cloud point pressure of additive in CO₂

The method of measuring cloud point pressure is used to determine the solubility of additives in CO₂, and the schematic diagram of the device for measuring the cloud point pressure of additives in CO₂ by photoresistor method is shown in Fig. 1. The experimental apparatus consists of a high-pressure view cell with a viewable window, a pressure monitoring system with an accuracy of ± 0.01 MPa, a temperature control system with an accuracy of ± 0.1 K, and a sampling system. There is sapphire glass on both sides of the high-pressure view cell, and the turbidity of the system in the high-pressure view cell can be quantified by the change in the resistance value of the photoresistor connected with the multimeter.

The resistance–pressure curve obtained from the measurements is shown in Fig. 2. With the decrease in pressure, the system gradually changes from a clear state to a turbid state. The turning point of the curve is the cloud point pressure. The detailed experimental procedures for measuring the cloud point pressure of additives in CO₂ are described in our previously published work and will not be repeated here (Lv et al., 2020).

2.2.2. Measurement of the IFT between CO₂ composite system and hexadecane

The experimental device for measuring the IFT between CO₂ composite systems and hexadecane is shown in Fig. 3. Hexadecane and CO₂ composite system were placed in two separate intermediate containers, driven by the ISCO pump and then entered the

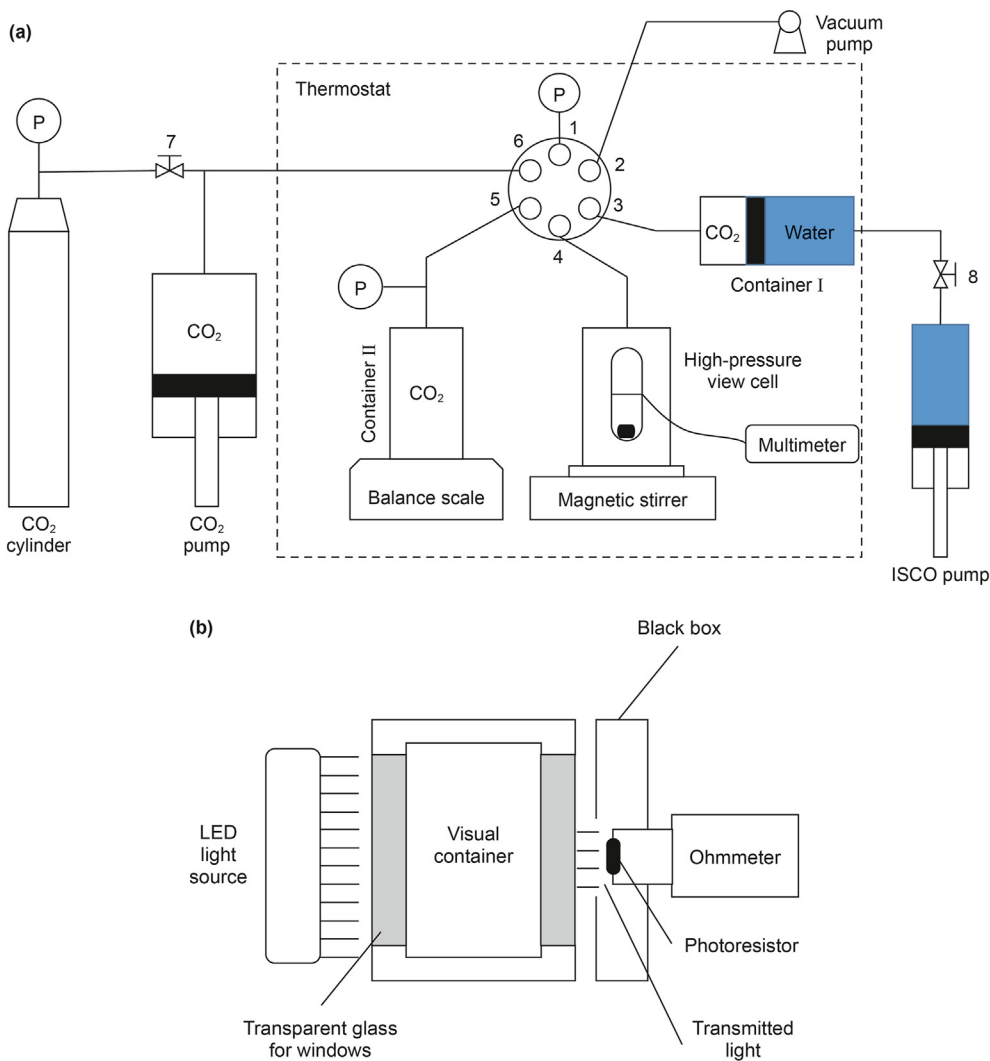


Fig. 1. Schematic diagram for measuring the cloud point pressure of additives. (a) Flowchart of the experimental setup, number 1–8 represent valves; (b) Schematic diagram of the measurement principle of the photoresistive method.

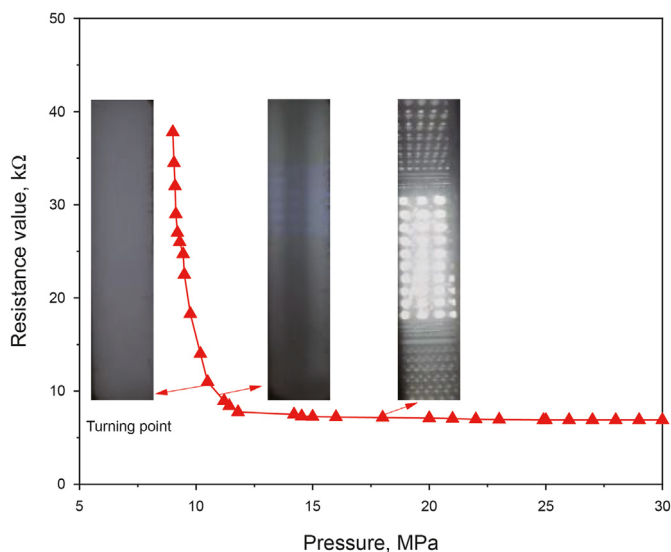


Fig. 2. Diagram of cloud point pressure measurement by photoresistor method (the curve represents the pressure–resistance change of 3.0% TTEG at 323 K).

hanging drop chamber. Then the shape of the oil droplets was recorded and measured by software. The detailed experimental procedures are described in our previously published work and will not be repeated here (Gong et al., 2024).

Here, the pendant drop method was used to measure the IFT between hexadecane and CO₂ composite systems. The droplet shape mainly depends on gravity and surface tension balance. Based on this idea, Andreas et al. (2002) proposed a simple calculation method, as shown in Eqs. (1) and (2). The image of the drop can be recorded by the data processing software and used to calculate the D_e and D_s of the droplet. Then the IFT can be calculated by inputting the density of hexadecane and CO₂ under the corresponding pressure.

$$\sigma = \frac{gD_e^2 \Delta\rho}{H} \tag{1}$$

$$S = \frac{D_s}{D_e} \tag{2}$$

where σ is the IFT, mN/m; g is acceleration gravity, m/s²; $\Delta\rho$ is the density difference between oil and CO₂ phases, g/cm³; D_e is the

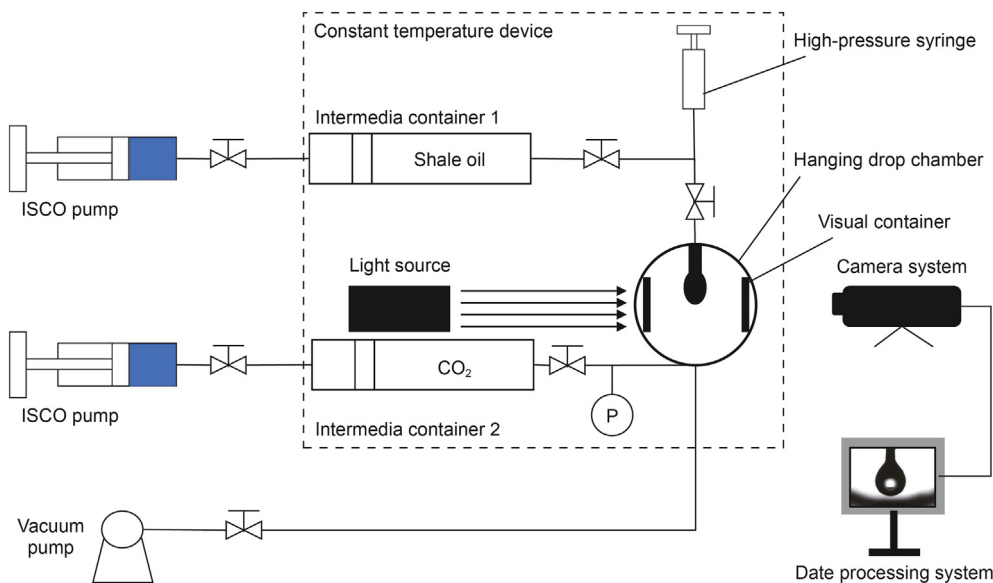


Fig. 3. Flow chart of the experimental equipment to measure the IFT between CO₂ and hexadecane.

diameter of the widest part of the droplet, mm; D_s is the diameter of the section that has a vertical distance D_e from the droplet top, mm; S is the shape factor; $1/H$ is the function of the droplet shape factor S .

2.2.3. Characterization of the extraction and expansion rates between CO₂ and hexadecane

A custom continuous evaluation device for the expansion and extraction rates of hexadecane with different pressures of CO₂ was used to study the behavior of hexadecane extraction and expansion in CO₂. As shown in Fig. 4, a customized inner tube with scale and side opening was added to the visual cell, and the transparent tube was equipped with a cap plug to prevent the hexadecane extracted by CO₂ from flowing back to the tube when the system pressure was reduced. A scaleplate was set on the side of the tube to accurately calculate the amount of remaining oil in the tube.

The experimental procedures are as follows:

(1) Under normal pressure, the hexadecane was dyed with a small amount of Sudan III. The pre-treated hexadecane with

the weight of m_0 was added to the inner tube with a stirrer, and its volume V_0 was measured.

- (2) The tube was put into the visual cell to insure that it can be seen completely from the view window of the visual cell.
- (3) The pipelines were connected and the whole system was vacuumed through the vacuum pump until the system pressure was less than 5.0 Pa.
- (4) Low-pressure CO₂ in the cylinder was transferred into the booster pump by opening valve 1; after pressuring in the booster pump, CO₂ went into the tank through valve 2. After several transfers, CO₂ in the tank can have a high pressure. The weight (g_1) of the tank and CO₂ can be recorded by the electronic scale.
- (5) CO₂ in the CO₂ gas tank was slowly added into the variable-volume view cell by opening valve 4. The weight of the tank and CO₂ can be recorded as g_2 .
- (6) The magnetic stirrer was opened. The oven power was turned on to control the temperature.
- (7) The cell pressure was controlled at P_0 through the ISCO pump. When the flow rate of the ISCO pump is 0, and the

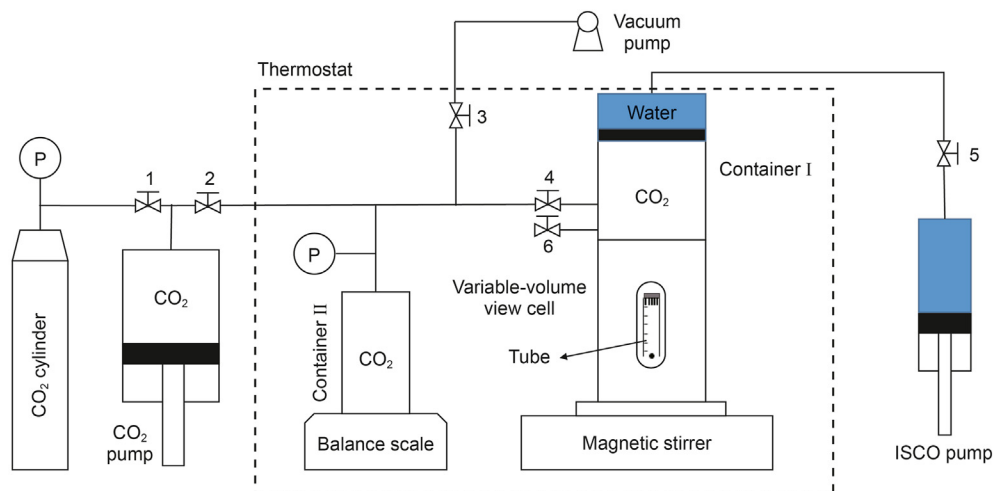


Fig. 4. Continuous evaluation device for the expansion and extraction rates of hexadecane in CO₂.

stability remains unchanged after 2 h, the system is considered stable. The volume V_{P_0} of the hexadecane in the tube was recorded. Valve 6 was opened, release the pressure slowly, and record the volume V_0' of the hexadecane in the inner tube after gas discharge.

- (8) Under the same conditions, hexadecane with the volume of V_0 and the weight of m_0 were injected according to steps (1)–(6), the ISCO pump was adjusted to keep the pressure of the cell stable at P_0 , and the volume V_{P_0} of hexadecane was recorded after equilibrium. The pressure was slowly increased to P_1 , the volume V_{P_1} of hexadecane after equilibrium was recorded, then the pressure was gradually reduced to P_0 , the volume of hexadecane at equilibrium was record as V_{P_0}' .
- (9) The pressure was sequentially increased to P_2 ($P_2 > P_1$), and the volume of hexadecane at equilibrium was recorded as V_{P_2} , then the pressure was slowly reduced back to P_1 , and the volume of hexadecane at equilibrium was recorded as V_{P_1}' .
- (10) Steps (8) and (9) were repeated until the system reaches miscibility.

The theoretical derivation is deduced as follows.

- (1) When the pressure is P_0 , the extraction amount is shown as follows:

$$V_{e,P_0} = V_0 - V_0' \quad (3)$$

The expansion amount can be calculated

$$V_{s,P_0} = V_{P_0} - (V_0 - V_{e,P_0}) = V_{P_0} - V_0' \quad (4)$$

The extraction rate of hexadecane for per unit mass of CO_2 at P_0 can be calculated by the following equation:

$$\alpha_0 = \frac{\rho_0(V_0 - V_0')}{m_0(g_1 - g_2)} \times 100\% \quad (5)$$

where ρ_0 is the density of hexadecane at 323 K.

The expansion rate of hexadecane for per unit mass of CO_2 at P_0 can be calculated by the following equation:

$$\beta_0 = \frac{V_{s,P_0}}{V_0 - V_{e,P_0}} \times \frac{1}{g_1 - g_2} \times 100\% \quad (6)$$

- (2) When the pressure is P_1 , the extraction amount is calculated as follows:

$$V_{e,P_1} = V_{e,P_0} + V_{P_0} - V_{P_0}' \quad (7)$$

The expansion amount is calculated from the following equation:

$$V_{s,P_1} = V_{P_1} - (V_0 - V_{e,P_1}) \quad (8)$$

The extraction rate of hexadecane for per unit mass of CO_2 at P_1 can be calculated by the following equation:

$$\alpha_1 = \frac{\rho_0 V_{e,P_1}}{m_0(g_1 - g_2)} \times 100\% \quad (9)$$

The expansion rate of hexadecane for per unit mass of CO_2 at P_1 can be calculated by the following equation:

$$\beta_1 = \frac{V_{s,P_1}}{V_0 - V_{e,P_1}} \times \frac{1}{g_1 - g_2} \times 100\% \quad (10)$$

- (2) When the pressure is P_2 , the extraction amount is calculated as follows:

$$V_{e,P_2} = V_{e,P_1} + V_{P_1} - V_{P_1}' \quad (11)$$

The expansion amount can be calculated

$$V_{s,P_2} = V_{P_2} - (V_0 - V_{e,P_2}) \quad (12)$$

The extraction rate of hexadecane for per unit mass of CO_2 at P_2 can be calculated by the following equation:

$$\alpha_2 = \frac{\rho_0 V_{e,P_2}}{m_0(g_1 - g_2)} \times 100\% \quad (13)$$

The expansion rate of hexadecane for per unit mass of CO_2 at P_2 can be calculated by the following equation:

$$\beta_2 = \frac{V_{s,P_2}}{V_0 - V_{e,P_2}} \times \frac{1}{g_1 - g_2} \times 100\% \quad (14)$$

- (4) According to Eqs. (2) and (3), it can be deduced the extraction and expansion rates of hexadecane.

When the pressure is P_i , the extraction amount is shown in the following equation:

$$V_{e,P_i} = V_{e,P_{i-1}} + V_{P_{i-1}} - V_{P_{i-1}}' \quad (15)$$

The expansion amount can be calculated as follows:

$$V_{s,P_i} = V_{P_i} - (V_0 - V_{e,P_i}) \quad (16)$$

The extraction rate of hexadecane for per unit mass of CO_2 at P_i can be calculated by the following equation:

$$\alpha_i = \frac{\rho_0 V_{e,P_i}}{m_0(g_1 - g_2)} \times 100\% \quad (17)$$

The expansion rate of hexadecane for per unit mass of CO_2 at P_i can be calculated by the following equation:

$$\beta_i = \frac{V_{s,P_i}}{V_0 - V_{e,P_i}} \times \frac{1}{g_1 - g_2} \times 100\% \quad (18)$$

3. Results and discussion

3.1. The cloud point pressure of glycol ether additives in CO_2

The cloud point pressure can reflect the affinity between the additives and CO_2 . When the cloud point pressure of the additive is low, it means that the additive is more likely to dissolve in CO_2 (Liu et al., 2002b; Lv et al., 2020; Zhu et al., 2018). The effects of mass fraction of glycol ether additive, temperature, and number of glycol groups on the cloud point pressure were investigated as well as the relationship between the solubility of additives and pressure.

3.1.1. The effects of mass fraction of glycol ether additive and temperature on the cloud point pressure

Fig. 5 shows the cloud point pressure of the three additives at different mass fractions and different temperatures. Under the same mass fraction, the cloud point pressure of DEG, TEG, and TTEG increases gradually with the increase in temperature. When the mass fraction of the additive is 2.0%, the variation range of DEG cloud point pressure is 8.3–9.8 MPa, the cloud point pressure of TEG is 8.4–11.4 MPa, and TTEG is 8.5–11.9 MPa. It can be seen that the cloud point pressure of TTEG increases significantly with the increase in temperature. Among the three additives, DEG has the lowest cloud point pressure, which may be related to the relatively poor CO₂ affinity of the glycol group (Lv et al., 2020). The molecular weight of DEG is the smallest, making it easily soluble in CO₂. Temperature affects the solubility of glycol ether additives in CO₂ in two opposite ways. On the one hand, with the increase in temperature, the density and the solvent force of CO₂ decrease and lead to the decrease in the solubility of additives in CO₂. On the other hand, the volatility of solute increases with the increase in temperature, which is conducive to the dissolution of additives in CO₂ (Liu et al., 2002a, 2002b). The density of CO₂ has a significant impact on the cloud point pressure of additives.

As the mass fraction of the additive increases, the cloud point pressure gradually increases. As the pressure of the CO₂ system increases gradually, the density of CO₂ also increases, enabling a greater amount of additive to be dissolved in CO₂. At 333 K, when the mass fraction of TTEG is 3.0%, the cloud point pressure is as high as 12.5 MPa. In other cases, the cloud point pressure of the three glycol ether additives with different temperatures and mass fractions is lower than 12.0 MPa. On the whole, the solubility of the three additives in CO₂ is high, which means that the additive can be dissolved in CO₂ in large quantities under a high pressure, and the synergistic mechanism can play a role in enhancing oil recovery.

3.1.2. The effect of the number of glycol groups on the cloud point pressure

The structure diagram of the three glycol ether additives is shown in Table 1. The three glycol ether additives are structurally similar but contain different numbers of glycol groups. In this part, the effect of the number of glycol groups on the cloud point pressure of the additives is investigated and compared with the alkyl block polyethers that have been reported (Lv et al., 2020). Fig. 6 shows the cloud point pressures of DEG, TEG, and TTEG with different mass fractions at 323 K. At the same mass fraction, when the number of glycol groups contained in the additive increases, the cloud point pressure of the additive shows an increasing trend. DEG has a small molecular mass, which has an unknown role in influencing the cloud point pressure. The effect of the molecular mass of the additive and the glycol group on the cloud point pressure was further analyzed.

Table 2 shows the cloud point pressures of different activities at 323 K. Among the three glycol ether additives, the CO₂+TTEG system has the highest molar fraction of glycol groups, and it can be seen that the molar fraction of glycol groups is positively correlated with the cloud point pressure. However, when the molar fraction of C₈(EO)₁₀ is 0.078% and the molar fraction of TTEG is 0.200%, the molar fraction of glycol groups contained in the two systems is approximately the same, but the cloud point pressure of C₈(EO)₁₀ is much higher than that of TTEG. This phenomenon indicates that additives with high molecular mass have relatively low solubility in CO₂ and the molecular structure of the additives has great influence on the dissolution of additive in CO₂.

The PO group has a higher affinity for CO₂ than the EO group (Liu et al., 2001; Ryoo et al., 2003). When the molar fraction of EO groups contained in CO₂+DEG system is approximately the same as

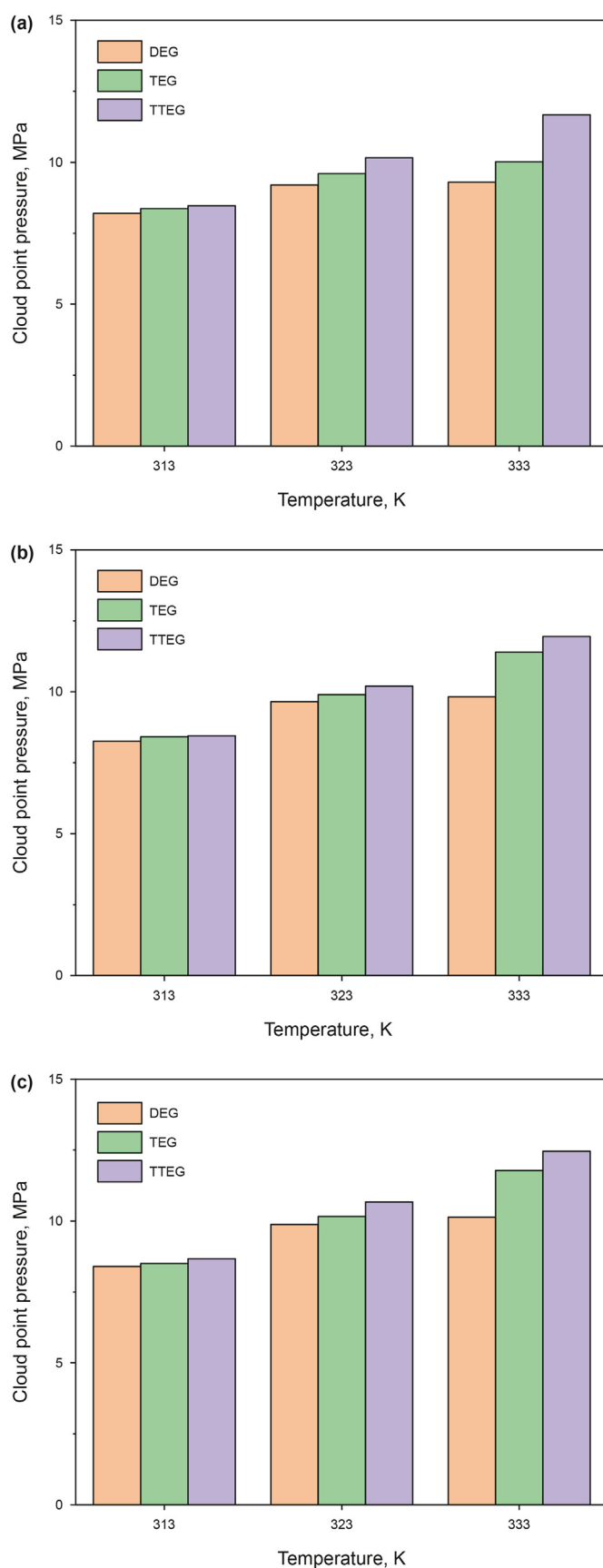
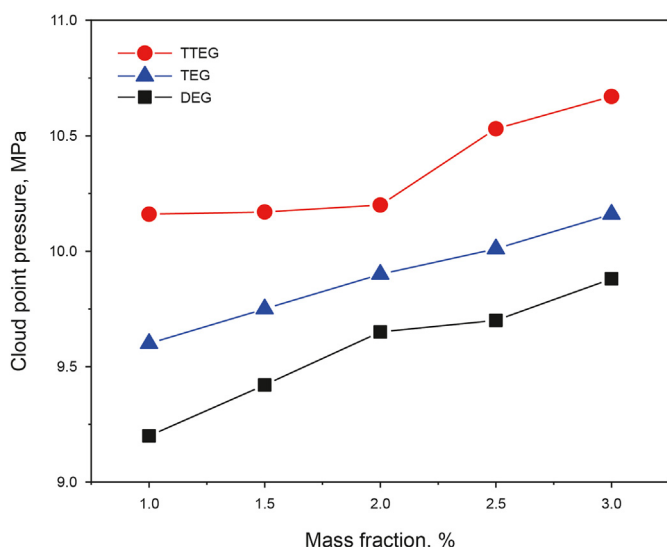


Fig. 5. Cloud point pressure diagrams of the three additives at different mass fractions and different temperatures. (a) 1.0%; (b) 2.0%; (c) 3.0%.

Table 1
Chemical structure formulas of DEG, TEG, TTEG, $C_m(\text{EO})_j$ and $C_m(\text{PO})_k$.

Name	Chemical formula structure
DEG	<chem>CH3-O-CH2-CH2-O-CH2-CH2-O-CH3</chem>
TEG	<chem>CH3-O-CH2-CH2-O-CH2-CH2-O-CH2-CH2-O-CH3</chem>
TTEG	<chem>CH3-O-CH2-CH2-O-CH2-CH2-O-CH2-CH2-O-CH2-CH2-O-CH3</chem>
$C_m(\text{EO})_j$	<chem>CH3-(CH2)_{m-2}-CH2-O-CH2-CH2-O-CH2-CH2-OH</chem>
$C_m(\text{PO})_k$	<chem>CH3-(CH2)_{m-3}-CH2-O-CH2-CH(CH3)-O-CH2-CH(CH3)-O-CH2-CH(CH3)-OH</chem>

**Fig. 6.** Cloud point pressures of DEG, TEG, and TTEG with different mass fractions at 323 K.

that of PO groups contained in $\text{CO}_2 + \text{C}_8(\text{PO})_{10}$ system, DEG with a lower molecular weight has a lower cloud point pressure. The comparison between $\text{C}_4(\text{PO})_3$ and the three glycol ether additives also shows that the molecular weight of the additives influences on the cloud point pressure. When screening additives, in addition to considering the type of CO_2 -philic groups in the additive, the molecular weight of the additive is also one of the important factors to be examined. For glycol ether additives, the number of glycol groups in the additive should not be excessive.

3.1.3. The relationship between the solubility of additives and cloud point pressure

When the pressure of the CO_2 +additive system reaches the

Table 2
Cloud point pressures of different activities at 323 K.

Name	Molecular weight, g/mol	Molar fraction of additive in the mixed system, mol%	Molar fraction of EO or PO groups in the system, mol%	Cloud point pressure, MPa
$\text{C}_8(\text{EO})_{10}$	570	0.078	0.780	23.8
$\text{C}_8(\text{PO})_{10}$	710	0.063	0.630	15.7
$\text{C}_4(\text{PO})_3$	248	0.179	0.537	10.1
DEG	134	0.330	0.660	9.2
TEG	178	0.249	0.747	9.6
TTEG	222	0.200	0.800	10.2

cloud point pressure of the additive, the additive can be completely dissolved in CO_2 . In oilfield development, the range of injection pressures for the CO_2 +additive system can be inverted from the solubility of the additive. Under a certain temperature and pressure, when the additive is completely dissolved in CO_2 , the solubility of additive in CO_2 is shown in Eq. (19).

$$x = \frac{m_a/M_a}{m_a/M_a + (V_g \rho_g/M_g)} \times 100\% \quad (19)$$

where x is the solubility of the additive in CO_2 ; m_a is the amount of additive, g; M_a and M_g represent the molecular mass of additive and CO_2 ; ρ_g represents the density of CO_2 at this temperature and pressure, g/cm^3 ; V_g represents the volume of CO_2 at this temperature and pressure, cm^3 .

The solubility of three glycol ether additives in CO_2 at different pressures are shown in Fig. 7. With the increase in system pressure, the dissolution ability of glycol ether additives in CO_2 increases greatly. At the same pressure, DEG has the highest solubility in CO_2 , indicating that DEG has the highest affinity with CO_2 , followed by TEG, and TTEG has the worst solubility in CO_2 . At 8.4 MPa and 313 K, the solubility of DEG in CO_2 can reach 1.000 mol%, while the solubility of TTEG is 0.199 mol%. The solubility of DEG is about 5 times that of TTEG, so the CO_2 +DEG system can be applied to lower formation pressures.

When the solubility of the three glycol ether additives in CO_2 is 0.500 mol%, the pressure of CO_2 at different temperatures is shown in Fig. 8. As can be seen, the cloud point pressure of DEG at the same temperature is the lowest among the three. When the temperature is 333 K, the cloud point pressure of DEG in CO_2 is 9.6 MPa, which is far lower than the reservoir rupture pressure and the miscible pressure of CO_2 and crude oil. Compared with DEG and TEG, TTEG can be dissolved in CO_2 at a higher pressure. Overall, all three glycol ether additives can be applied to reservoirs with low formation pressures, and the additives are less likely to precipitate out of the CO_2 during the process of injection into the formation with the CO_2 .

3.2. Effects of glycol ether additives on the IFT between CO_2 and hexadecane

During CO_2 flooding or huff-n-puff process, the oil and CO_2 interface will be present when the oil and CO_2 cannot be miscible. The IFT between oil and CO_2 can influence the two-phase flow and the oil recovery during the flow process. The effect of glycol ether additive on the IFT between CO_2 and hexadecane has been investigated here.

3.2.1. The IFT between CO_2 and hexadecane

The IFT between CO_2 and hexadecane at different pressures was measured, and the minimum miscible pressure (MMP) of CO_2 and hexadecane was determined by the interfacial tension method (Zhang et al., 2019). Fig. 9 shows the IFT between hexadecane and CO_2 at different pressures at 323 K. It can be seen that the IFT between hexadecane and CO_2 is divided into two stages, and in the

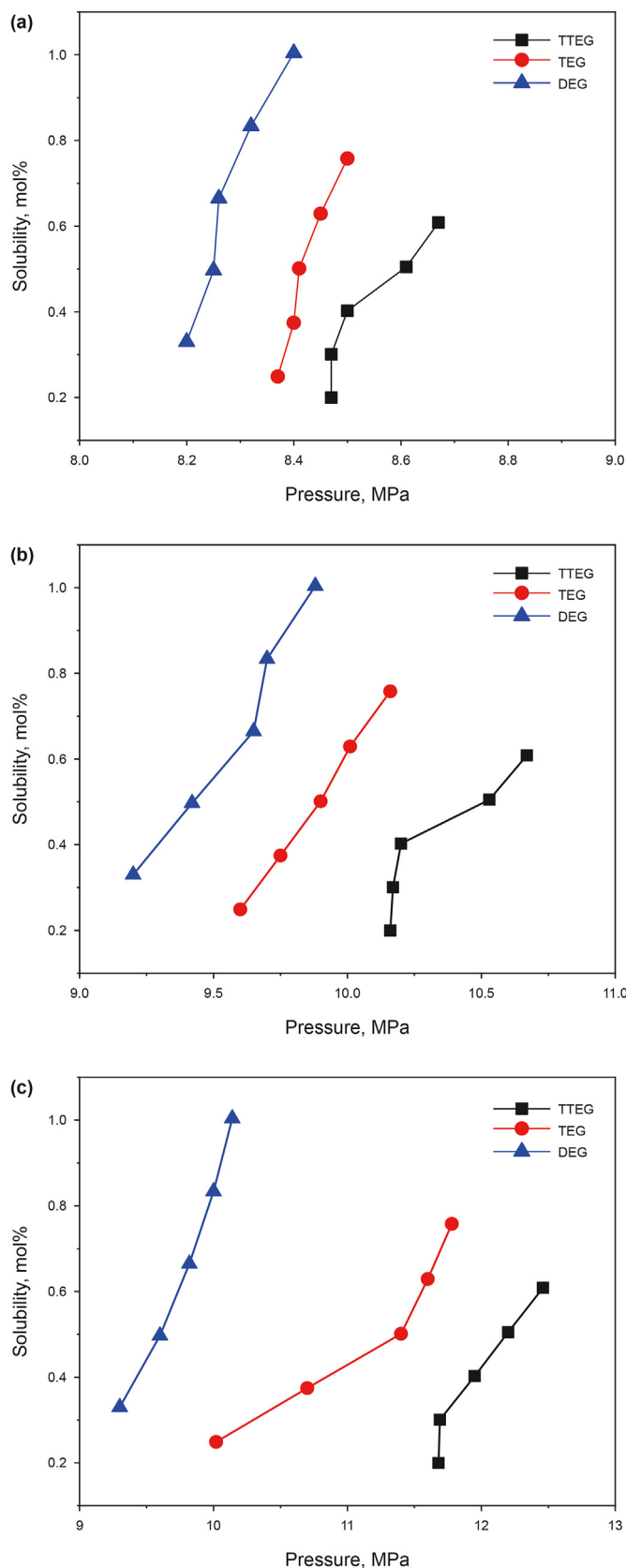


Fig. 7. The relationship between the solubility of the additive in CO₂ and the pressure at different temperatures. (a) 313 K; (b) 323 K; (c) 333 K.

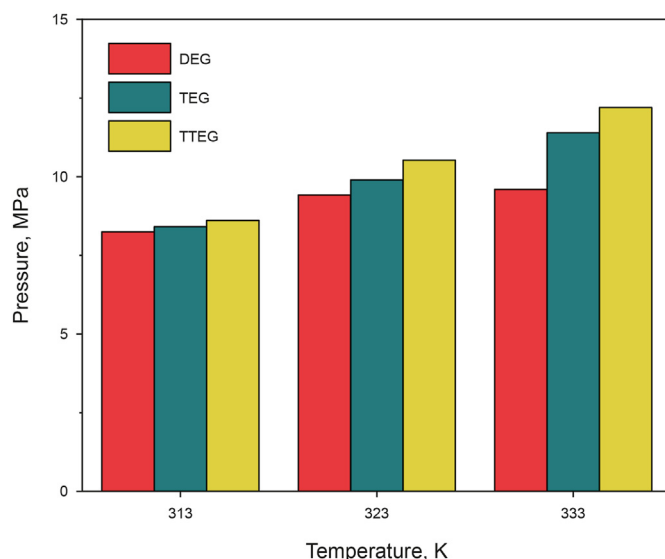


Fig. 8. Cloud point pressure of three ether additives with the same solubility of 0.500 mol%.

first stage, the IFT decreases rapidly with the increase in pressure, as shown in line A, which is directly related to the rapid increase in the density of CO₂ (Wang et al., 2018). In the second stage, as the pressure rises, the IFT decreases slowly. CO₂ is in the supercritical state, and the change of density is no longer obvious. There is mass exchange between CO₂ and hexadecane, and the mutual diffusion effect leads to the gradual disappearance of the interface between them. By fitting the line B, the MMP of CO₂ with hexadecane was deduced to be 17.24 MPa.

The droplet shapes of hexadecane in CO₂ under different pressures were measured and shown in Fig. 10. It can be seen that the droplet shape of hexadecane in CO₂ is a full pear-shape when the pressure is low. The droplet gradually changes from a pear-shape to an oval-shape with the increase of pressure. When the pressure reaches 10.0 MPa, it can be found that the droplet slowly shrinks. As the pressure approaches MMP, the hexadecane is no longer able to converge into droplets, indicating that the IFT between CO₂ and hexadecane is already at a low value. It can also be found that the volume of the oil droplets first increases and then decreases with the increase in pressure, which is related to the extraction and expansion of CO₂. At lower pressures, CO₂ gradually dissolves in the oil, resulting in expansion of the oil droplet volume, while with the increase in pressure, the extraction effect of CO₂ on the oil is more obvious and the oil droplet volume gradually decreases. This phenomenon was also reported by Li et al. (2016). In the porous media of reservoirs, if additives can enhance the extraction and expansion effects of CO₂, it is beneficial for reducing the IFT between CO₂ and crude oil and improving oil recovery.

3.2.2. Effects of different additives on the IFT between CO₂ and hexadecane

The effects of different additives on reducing the IFT between CO₂ and hexadecane at different pressures were analyzed. Ethanol as a common additive is effective in reducing the IFT between CO₂ and crude oil as well as improving recovery (Saira et al., 2021; Zhang C. et al., 2020). Glycol ether additives were compared to ethanol in this part. The droplet shape of hexadecane in CO₂ after adding different additives under different pressures was shown in Fig. 11. With none additives, the oil droplet volume decreases gradually with the increase in pressure, however, after the addition

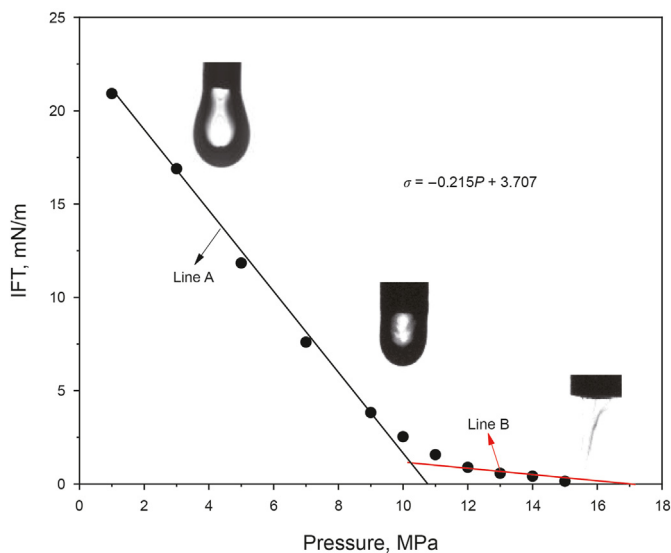


Fig. 9. The IFT between hexadecane and CO₂ at different pressures at 323 K.

of ethanol and glycol ether additives, the oil droplet volume decreases significantly. Among the three glycol ether additives, DEG has the greatest impact on the shape of hexadecane droplets. At the pressure of 13.0 MPa, droplets fail to coalesce in CO₂+DEG system, suggesting that the IFT between the hexadecane–CO₂ system is already at a low value, however, hexadecane can still converge into tiny droplets in CO₂+TEG system. TTEG has less effect on the volume of oil droplets, suggesting that it is not as effective as DEG and TEG in reducing the IFT between CO₂ and hexadecane. The effect of ethanol on oil droplet volume is weaker than that of DEG. From the point of view of oil droplet volume change, it can be seen that low molecular weight glycol ether additives have beneficial effects in promoting the extraction of CO₂.

Fig. 12 shows the IFT between hexadecane and CO₂ under different pressures after adding different additives. With the increase in pressure, the IFT between hexadecane and CO₂ decrease gradually. Adding additives can all decrease the IFT. Nevertheless, at the same pressure, the IFT between hexadecane and CO₂+DEG system is the lowest. The IFT between hexadecane and CO₂ system in the presence of ethanol and TEG are slightly higher than that of DEG. Additionally, when the pressure reaches 13.0 MPa, the hexadecane ceases to form droplets, making it impossible to calculate the IFT.

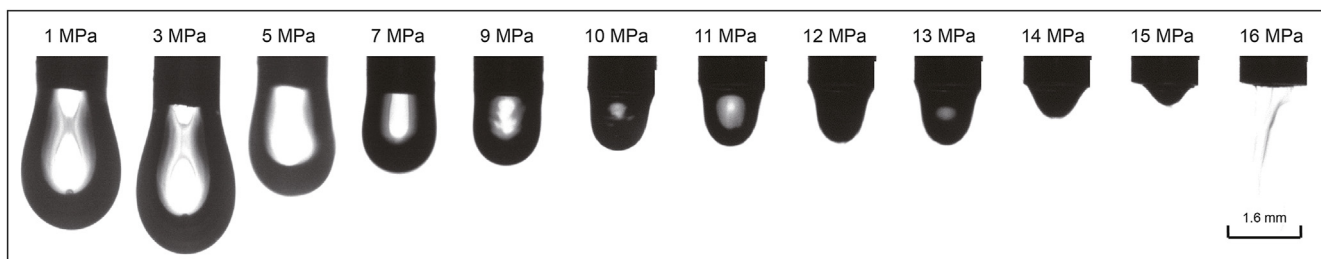


Fig. 10. Droplet shapes of hexadecane in CO₂ under different pressures at 323 K.

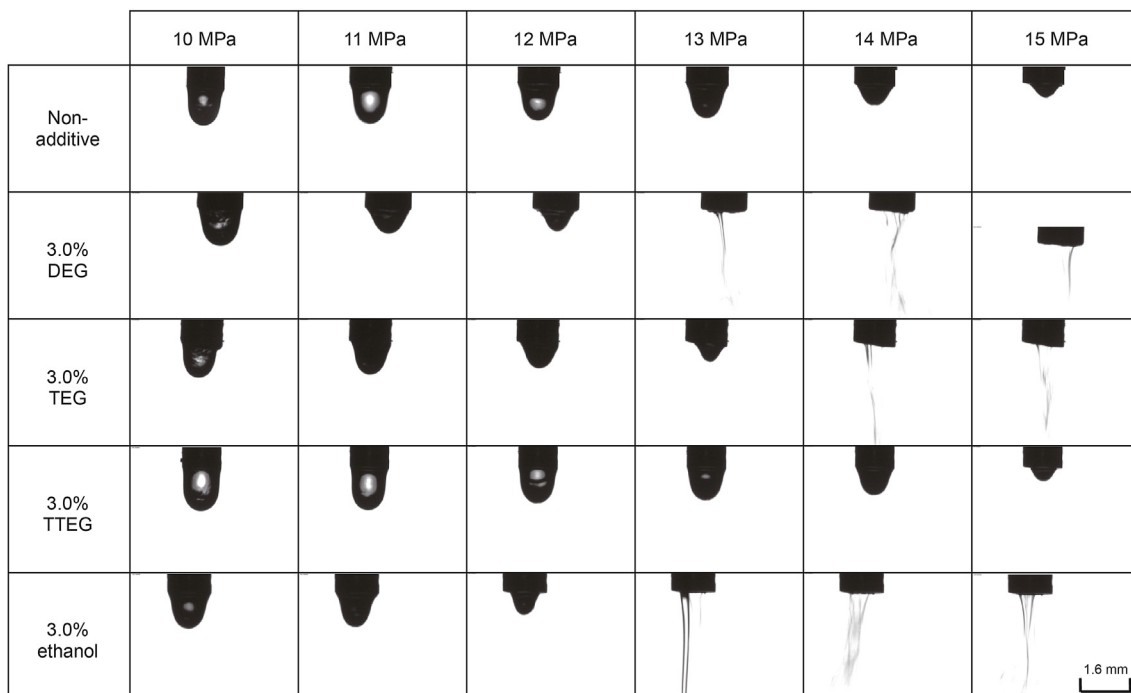


Fig. 11. Droplet morphology of hexadecane in CO₂ after adding different additives at 323 K.

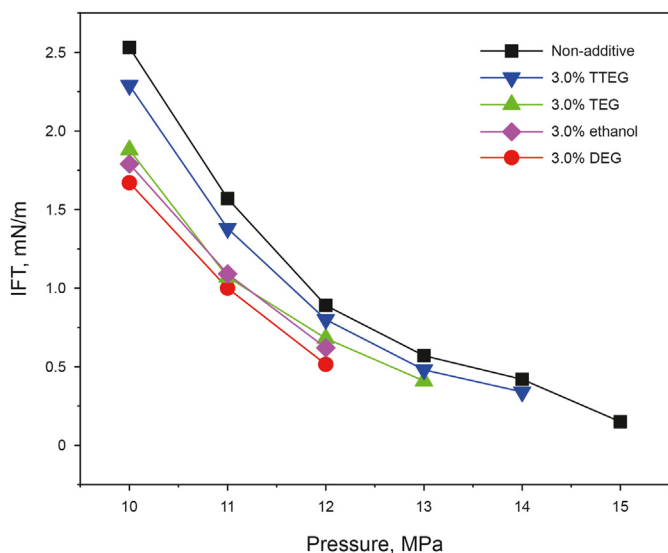


Fig. 12. The IFT between hexadecane and CO₂ under different pressures after adding different additives.

Table 3 shows the MMP of hexadecane and CO₂+additives system and Table 4 shows the degree of reduction in the IFT between hexadecane and CO₂ under different pressures. The addition of DEG can decrease the IFT between hexadecane and CO₂ by 40.0%, and MMP by 25.5% down to 12.8 MPa. Ethanol can lower the IFT between hexadecane and CO₂ by 30.0%, and MMP by 24.6% down to 13.0 MPa. The impact of TEG is slightly weaker than that of ethanol, while the effect of TTEG is the worst, reducing the IFT between hexadecane and CO₂ by less than 20.0%, and decreasing MMP by only 11.0%.

On the whole, the addition of glycol ether additive can significantly decrease the IFT and MMP of hexadecane and CO₂. The reasons are as follows. Firstly, the density of the CO₂+glycol ether additive system is further increased compared with CO₂, resulting in a decrease in the density difference between the CO₂ system and hexadecane (Wang et al., 2018). Secondly, the addition of glycol ether additives can be spread on the surface of CO₂ and hexadecane, which is beneficial for mutual diffusion between hexadecane and CO₂ (Gong et al., 2024). Additionally, the relative molecular weight

Table 3
The MMP of hexadecane and CO₂ with different additives.

Additive	Fitted line	MMP, MPa	Reduction, %
Non-additive	$\sigma = -0.215P + 3.707$	17.24	/
3.0% DEG	$\sigma = -0.577P + 7.414$	12.84	25.52
3.0% TEG	$\sigma = -0.330P + 4.680$	14.18	17.75
3.0% TTEG	$\sigma = -0.230P + 3.530$	15.34	11.02
3.0% ethanol	$\sigma = -0.585P + 7.602$	12.99	24.65

Notes: σ is the IFT, mN/m; P is the pressure, MPa.

Table 4
Reduction degree of IFT between hexadecane and CO₂ under different pressures with different additives.

Pressure, MPa	IFT reduction degree, %			
	3.0% DEG	3.0% TEG	3.0% TTEG	3.0% ethanol
10.0	33.99	25.69	9.49	29.25
11.0	36.31	31.85	12.10	30.57
12.0	41.57	23.60	10.11	30.34
13.0	/	28.07	15.79	/
14.0	/	/	19.05	/

of glycol ether additive is similar to that of hexadecane, increasing the polarity of the CO₂ system, thereby increasing the interaction force between CO₂ and hexadecane.

Table 4 also shows that the effectiveness of the glycol ether additives in reducing the IFT between CO₂ and oil gradually increases with the increase in pressure. When the pressure increases, the additive is less likely to separate from CO₂ and the additive and CO₂ system is more stable.

3.2.3. The effect of additive concentration on the IFT between CO₂ and hexadecane

Among the three additives, DEG exhibited the most significant reduction in IFT and displayed the best solubility in CO₂. The effect of the concentration of DEG on the IFT between CO₂ and hexadecane was further investigated. Fig. 13 shows the shape of oil droplets in CO₂ after adding different concentrations of DEG. With the addition of DEG additive, there is a significant change in droplet volume that can be observed, and as the mass fraction of the additive increases, the droplet volume gradually decreases under the same pressure. Additionally, without the addition of additives, hexadecane can still form small droplets at the pressure of 15.0 MPa; when the mass fraction of DEG is 1.0%, droplets cannot be formed at the pressure of 14.0 MPa; and when the mass fraction is 3.0%, small droplets cannot be formed at the pressure of 13 MPa. As the amount of DEG increases, the size of the droplets gradually decreases. DEG disperses at the interface of CO₂ and hexadecane, which enhances the diffusion and mass transfer between them. In addition, DEG enhances the extraction of CO₂ and promotes the CO₂ and hexadecane miscibility.

Fig. 14 quantitatively calculates the IFT and the decrease of IFT after adding different mass fractions of DEG under different pressures. It can be observed that as the DEG mass fraction increases, the IFT between the hexadecane and CO₂ gradually decreases.

At the pressure of 12.0 MPa, the mass fraction of 3.0% DEG can reduce the IFT by 40.0%. Furthermore, adding 1.0% of DEG in CO₂ can reduce the IFT by about 20.0%, highlighting the great potential of DEG for further application.

3.3. Effect of DEG on the extraction and expansion behavior between CO₂ and hexadecane

The extraction and expansion performance of CO₂ on crude oil is one of the main mechanisms of oil displacement (Han et al., 2015). The effect of CO₂ on hexadecane extraction and expansion behavior was studied. A custom continuous evaluation device for the expansion and extraction rates of oil and CO₂ was used to quantitatively analyze the extraction and expansion behavior between CO₂ and hexadecane under different pressures. The mass of each component in different systems are as shown in Table 5.

3.3.1. The extraction and expansion performance of CO₂ and hexadecane under different oil–gas ratios

In this part of the experiment, the extraction and expansion of CO₂ on hexadecane were studied by setting different oil–gas ratios. Based on the experimental setup shown in Fig. 4, the volume of hexadecane at different pressures can be calculated, thereby determining the extraction and expansion amounts of CO₂ on hexadecane. To control a single variable, when the mass fraction of hexadecane is 5.0% and 3.9%, the mass of CO₂ in the CO₂+hexadecane system is kept constant, and when the mass fraction of hexadecane is 3.9% and 3.2%, the mass of hexadecane is kept constant. Fig. 15 shows the volume change of hexadecane with the mass fraction of 5.0%. Fig. 16 shows the volume change of hexadecane with different mass fractions at various equilibrium times.

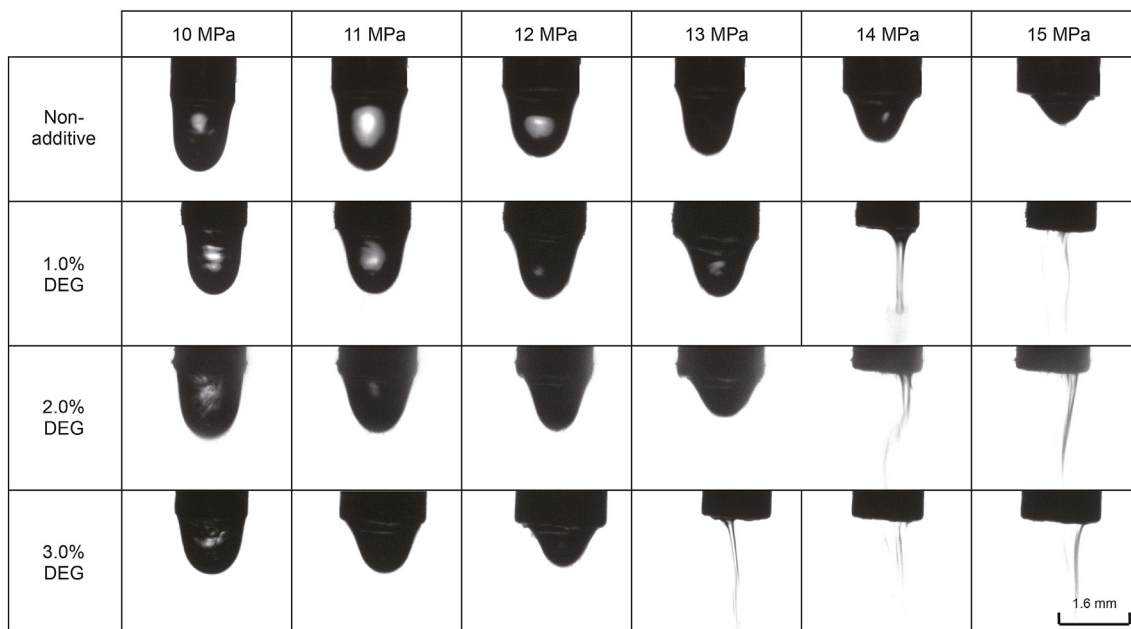


Fig. 13. Droplet shape of hexadecane in CO₂ after adding different concentrations of DEG at 323 K.

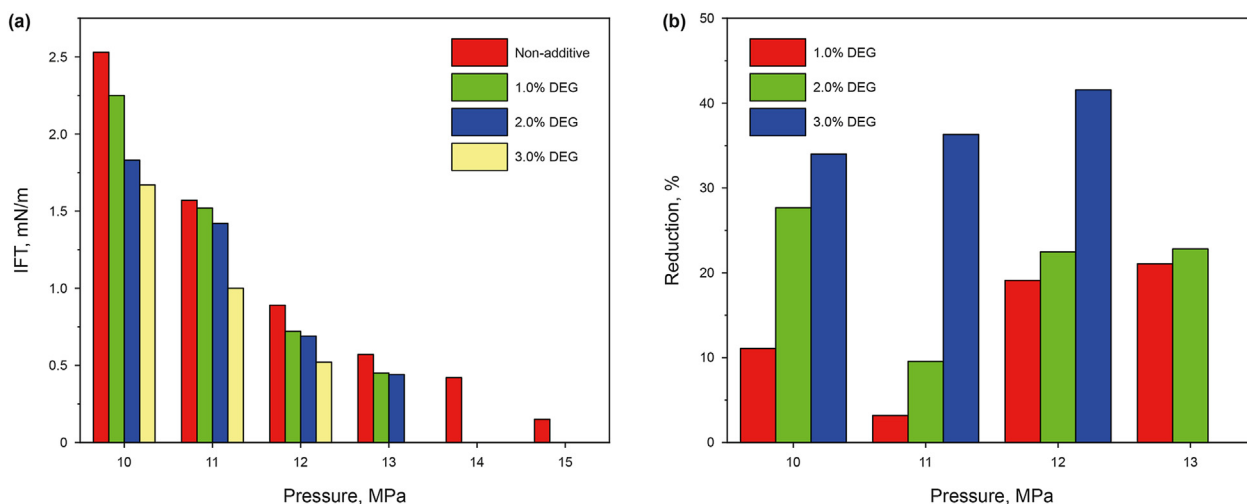


Fig. 14. The IFT between hexadecane and CO₂ (a) and reductions of IFT (b) after adding different mass fractions of DEG at 323 K.

Table 5

The mass of each component in different systems.

Mass fraction of hexadecane, %	Hexadecane mass, g	CO ₂ mass, g	DEG mass, g
5.0	3.684	70.200	0
3.9	2.841	70.000	0
3.2	2.844	85.900	0
5.0	3.687	70.100	0.700

By means of a reciprocating process of pressurization and depressurization, the extraction and expansion volumes of hexadecane at different pressures can be continuously calculated. It can be found that the oil volume increased when the pressure was increased to 8.0 MPa at 6 h from the original stage, and further increased when the pressure was increased to 9.5 MPa at 12 h. When the pressure was decreased to 8.0 MPa, the volume at 18 h was lower than that at 6 h because of the extraction effect. When

the pressure was further increased to 11 MPa, the oil volume at 24 h increased again. Although a portion of hexadecane has been extracted, the volume of the hexadecane at 24 h is more than that at 12 h, which is due to the stronger expansion effect of CO₂ at lower pressures compared to the extraction effect (Li et al., 2016). As the pressure was decreased to 9.5 MPa, the volume at 30 h is lower than that at 18 h. However, when the pressure was further increased to 12.5 MPa, the volume was not further increased but decreased

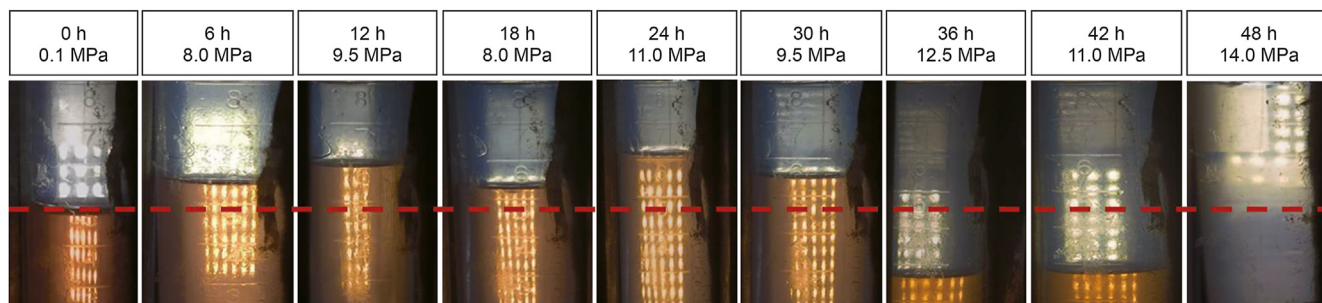


Fig. 15. The volume change of hexadecane with the mass fraction of 5.0% at different stages (6 h is the equilibrium time under a set of pressures).

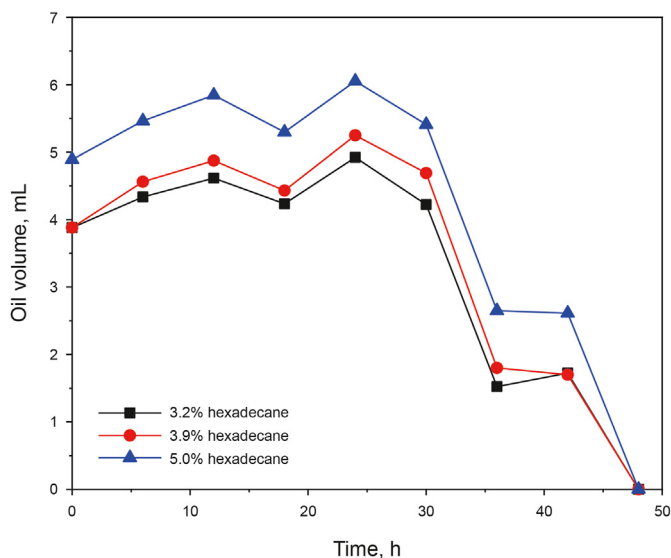


Fig. 16. Volume change of hexadecane with different mass fractions in the inner tube at different stages.

greatly at 36 h. This is due to the strong extraction effect at 12.5 MPa to extract more oil into CO₂ phase. As the pressure was decreased back to 11.0 MPa, the left oil is much less than that at 24 h, which is also due to the strong extraction effect. When the pressure was increased to 14.0 MPa, there is no oil phase left in the inner tube, CO₂ and hexadecane have already reached a complete miscibility state.

Fig. 16 shows that when the mass fraction of hexadecane is higher, the volume of hexadecane is relatively larger at different pressures. At the molecular level, when the solubility of CO₂ in hexadecane is low, hexadecane molecules tend to bend and intertwine with each other. However, as the solubility of CO₂ in hexadecane increases, the hexadecane molecules become more extended, and CO₂ molecules fill the gaps between the hexadecane molecules. This results in an expansion of the volume of hexadecane (Liu et al., 2015). Although the initial volume of hexadecane is the same when the mass fraction is 3.2% and 3.9%, the latter has a larger volume than the former at different pressures, suggesting that when the oil–gas ratio increases, CO₂ can be more effectively utilized. Overall, the volume of hexadecane exhibits a trend of initial increase followed by decrease, and at different pressure stages, the extraction and expansion effects of CO₂ are not the same.

In conventional measurement method, CO₂ and oil are loaded into the PVT instrument to study the expansion effect of CO₂ on the oil (Han et al., 2015; Li et al., 2013; Wei et al., 2017). The swelling

factor is calculated by the ratio of the expanded-oil volume to the original-oil volume. In fact, the oil volume can be decreased due to the extraction effect, and it is not the real volume of oil before the expansion effect. The calculated swelling factor decreases greatly when the pressure increases to a certain value. The decrease in the swelling factor is not due to the reduction of the expansion effect and the real reason is the decrease in oil volume caused by the extraction effect. The phenomenon cannot really reflect the extraction and expansion effect especially at high pressures because the extraction and expansion effects are occurring simultaneously and cannot be distinguished by the conventional experimental methods.

Ding et al. (2019) has improved the calculation method for the extraction and expansion effects of CO₂ and oil by injecting CO₂ multiple times into the intermediate container filled with crude oil and discharging the gas mixture of CO₂ and oil, thereby calculating the extraction amount. In this work, the extraction and expansion effects are distinguished by a novel experiment design. The extraction and expansion amounts of CO₂ and oil under different pressures can be measured and quantitatively calculated. Meanwhile, the phase behavior changes of CO₂ and oil can be observed through the window of the visual instrument.

The swelling factor of hexadecane under different pressures calculated by method of this work and the conventional method is shown in Fig. 17. It can be seen that with the increase in pressure, the swelling factor calculated by the conventional method first

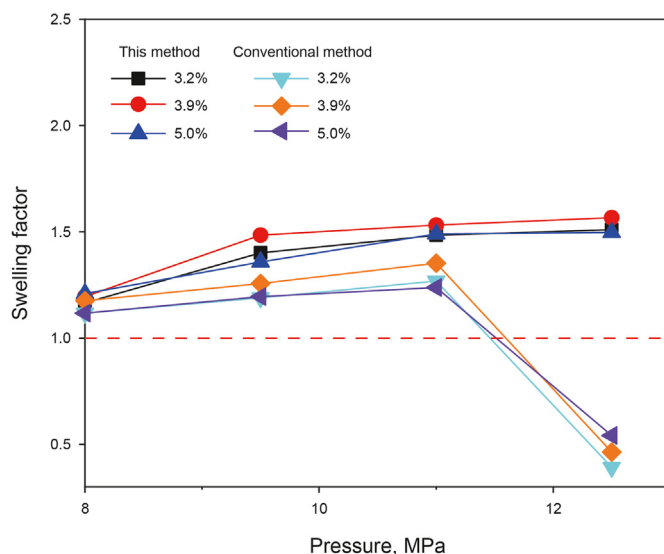


Fig. 17. Swelling factor of hexadecane with different mass fractions under different pressures calculated by different methods at 323 K.

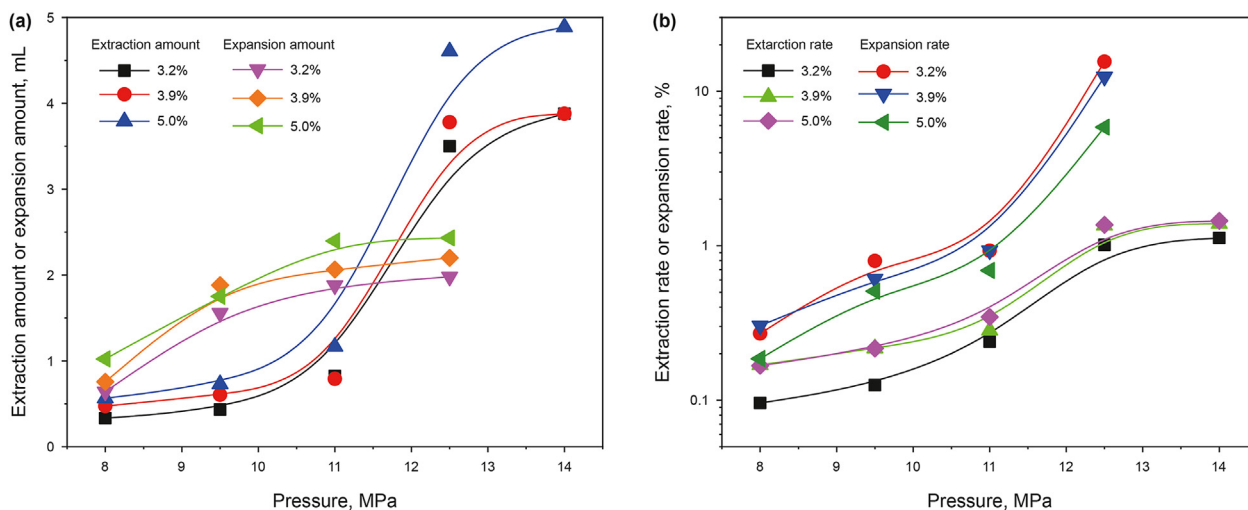


Fig. 18. Extraction and expansion behavior of hexadecane by CO_2 under different pressures and different mass fractions. (a) Extraction and expansion amounts; (b) Extraction and expansion rates.

increases and then decreases to lower than 1. However, the swelling factor calculated by this method is always greater than 1 and gradually increases, which can clarify the strong expansion effect at high pressures. Conventional measurement methods do not account for the impact of CO_2 extraction on the oil volume.

The extraction and expansion amounts of CO_2 on hexadecane under different mass fractions and different pressures were calculated and shown in Fig. 18(a). With the increase in pressure, both the extraction and expansion amounts gradually increase. The difference is that the expansion amount increases in the form of exponent, while the extraction amount increases in the shape of “S”.

The extraction and expansion effects can be divided into three stages. In the first stage, at lower pressures, CO_2 gradually dissolves in the oil and exerts a more significant expansion effect on the oil, yet the extraction effect is relatively weak. With the increase in pressure, the expansion amount grows rapidly, while the extraction amount increases slowly. In the second stage, the molecular thermal motion and the diffusion between CO_2 and hexadecane is gradually enhanced. The oil gradually diffuses from the oil phase into the gas phase, and the extraction is stronger than the expansion. During this stage, the extraction amount increases rapidly and even counteracts the expansion amount, while the expansion amount gradually stabilizes. At the third stage, there is very little hexadecane in the oil phase, most of the hexadecane has diffused into the CO_2 phase. When the system pressure is 14.0 MPa, hexadecane and CO_2 are completely mixed.

The oil–gas ratio affects the extraction and expansion effects of CO_2 , at the same pressure, the expansion and extraction effects are enhanced with the increase in the mass fraction of hexadecane. The extraction and expansion rates of per unit mass CO_2 for hexadecane was further investigated. Fig. 18(b) shows that the extraction rate and expansion rate all increase with the increase in pressure and the expansion rate is always higher than the extraction rate in the full range of pressures.

When the pressure is lower than 11.0 MPa, both the expansion rate and extraction rate increase with the increase in pressure slowly. When the pressure is larger than 11.0 MPa, the expansion rate increases greatly, while the extraction rate increases gradually to a stable value. As shown in Eqs. (17) and (18), the extraction rate of per unit mass CO_2 is mainly affected by the extraction amount, while the expansion rate of per unit mass CO_2 is influenced by the

volume of oil remaining in the pipe and the extraction amount. Therefore, as the mass fraction of hexadecane increases, the extraction rate gradually increases, while the expansion rate decreases due to the influence of the extraction amount.

3.3.2. Effect of 1.0% DEG on the extraction and expansion effects of CO_2 and hexadecane

The extraction and expansion effects between oil and CO_2 can enhance the interactions between oil and CO_2 and enhance the oil recovery. DEG has high solubility in CO_2 and can significantly reduce the IFT between CO_2 and oil. In this part, the influence of DEG on the extraction and expansion performance of hexadecane and CO_2 was investigated and shown in Fig. 19.

As 1.0% DEG was added into the CO_2 and oil system, the extraction and expansion behavior has great changes. When the pressure is at 8.0 or 9.5 MPa, the extraction amount and extraction rate of the composite system have greater decreases while the expansion amount and expansion rate have more obvious increases than the parameters of the CO_2 and oil system. This is because that the pressure has not reached the cloud point pressure of DEG in CO_2 , CO_2 has dissolved some parts of DEG, and cannot extract more oil. When the pressure increases to 11.0 MPa, the extraction and expansion effects both have great enhancement in the presence of DEG. At 11.0 MPa, the expansion amount of 1.0% DEG was 1.75 times that of the expansion amount without additives, and the extraction amount of 1.0% DEG was 2.25 times that of the extraction amount without additives. The results mean that the dissolution of DEG in CO_2 can accelerate the extraction effect of oil into CO_2 and meanwhile the dissolution of DEG in oil can enhance the expansion of oil due to the increase in CO_2 molecules dissolved in oil. DEG molecules can simultaneously dissolved into oil and CO_2 to enhance the extraction and expansion effects due to the CO_2 -philic and lipophilic property.

3.3.3. The mechanism of DEG-enhanced extraction and expansion

The mechanism of DEG-enhanced extraction and expansion actions of CO_2 was further analyzed and shown in Fig. 20. Fig. 20(a) shows the schematic diagram of the extraction and expansion effects of CO_2 and oil without additives at different pressure stages. In the first stage, when the pressure is low, some CO_2 molecules dissolve in the oil, and the expansion effect is stronger than the extraction effect. With the increase in pressure, the amount of

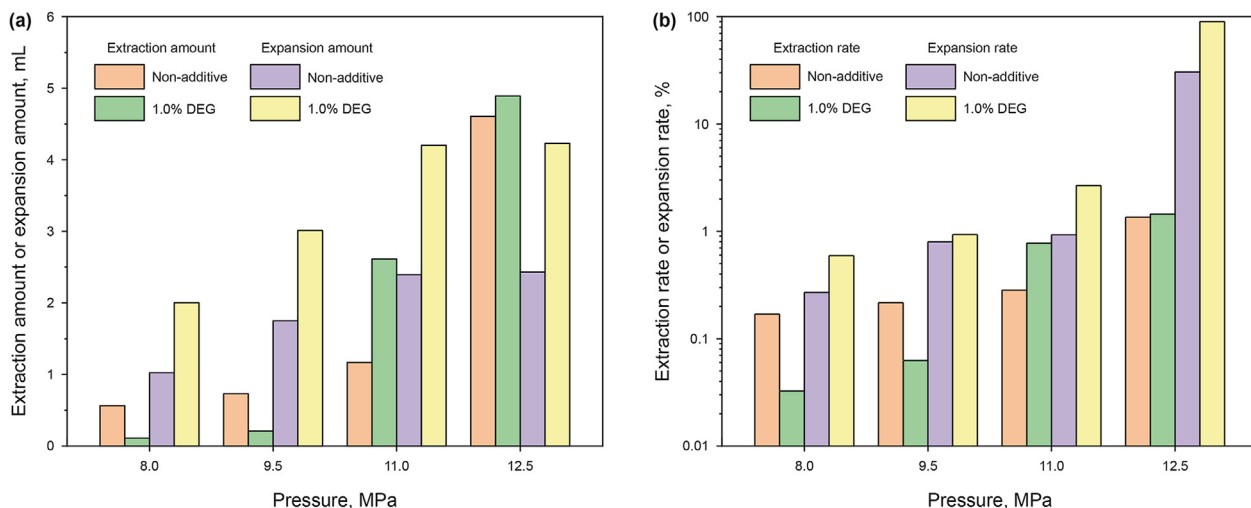


Fig. 19. Effect of 1.0% DEG on the extraction and expansion effects of CO₂ and hexadecane. (a) Extraction and expansion amounts; (b) Extraction and expansion rates of hexadecane induced by CO₂ per unit mass.

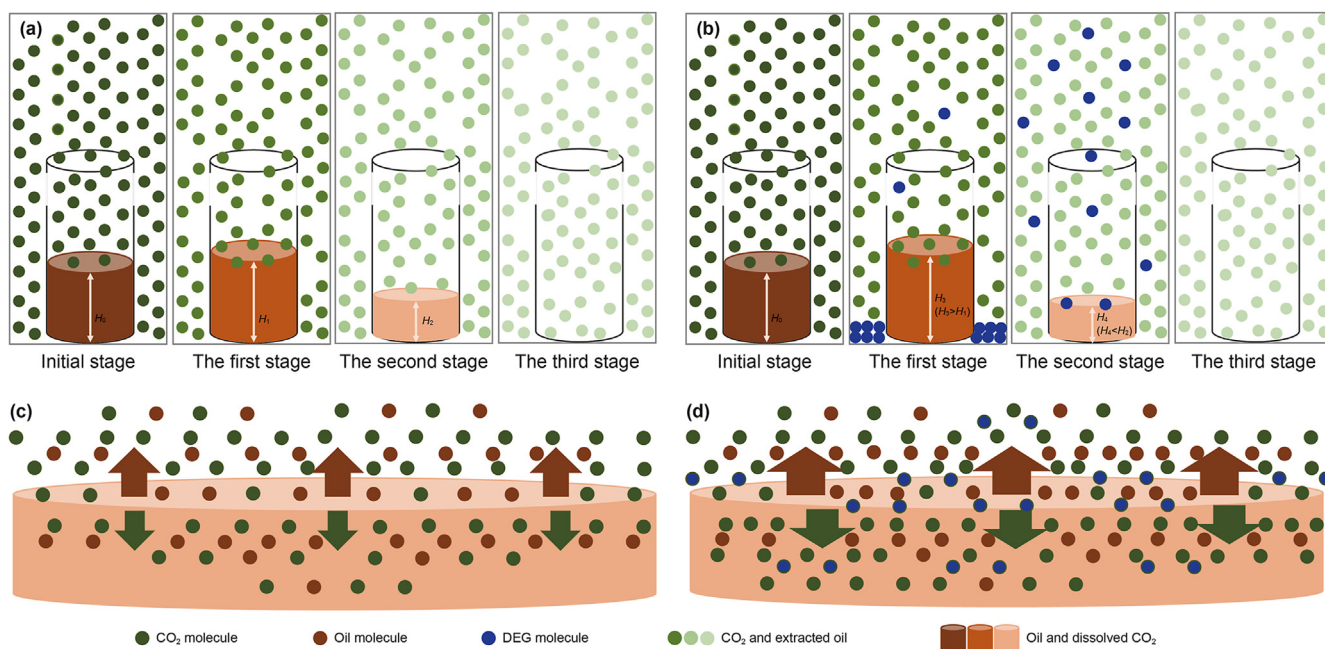


Fig. 20. Schematic diagrams of the extraction and expansion effects of CO₂ at different pressure stages (the gradation of color represents the miscibility degree of CO₂ and oil.). (a) Without additives; (b) Adding additives; (c) Interface schematic of CO₂ and oil in the third stage without additives; (d) Interface schematic of CO₂ and oil in the third stage after adding additives. H₀, H₁, H₂, H₃, and H₄ are the liquid level heights of the oil at different stages.

extracted oil gradually increases due to the strong mass transfer and diffusion effects between CO₂ and oil, leading to a reduction in the volume of the oil. In the third stage, the extraction effect of CO₂ becomes more significant, with all the oil being extracted into the CO₂ phase. At this time, CO₂ and oil have completely mixed into a single phase.

Fig. 20(c) shows the interface schematic of CO₂ and oil in the third stage without additives. It can be seen that there is a strong diffusion effect between CO₂ molecules and oil molecules. The CO₂ molecules diffuse into the oil phase, promoting the expansion of the oil, and due to the extraction effect of CO₂, a large number of oil molecules enter the CO₂ phase due to the enhancing of the miscibility between CO₂ and oil with the increase in pressure.

After the addition of additives, as shown in Fig. 20(b), when the

pressure is lower than the cloud point pressure of the additives, a small amount of additives dissolves in the CO₂. The additives have a certain polarity and stronger interaction forces with oil molecules, which can promote the dissolution of CO₂ in the oil. Therefore, the volume of the oil will increase during the first stage. When the pressure is higher than the cloud point pressure of the additives, the additives are completely dissolved in the CO₂, which enhances the extraction and expansion effects of CO₂. At this time, the extraction effect of CO₂ is stronger, causing a significant reduction in the volume of the oil. As the pressure continues to rise, CO₂ and oil completely mixed into a single phase. Fig. 20(d) shows the interface schematic of CO₂ and oil in the third stage after adding additives. DEG molecules have good affinity with CO₂, and due to the stronger polarity of DEG, there are also strong interaction forces

between DEG and oil molecules. Therefore, DEG molecules tend to spread at the interface between oil and CO₂, which enhances the diffusion effect between CO₂ molecules and oil molecules. As a result, more CO₂ molecules dissolve in the oil, and more oil molecules are extracted into the CO₂ phase along with CO₂ molecules, promoting the miscibility between CO₂ and oil. Improving the extraction and expansion effects of CO₂ is beneficial for enhancing oil recovery.

4. Conclusions

In this paper the solubility of three glycol ether additives in CO₂ and the influence of these additives on the interactions between CO₂ and hexadecane were investigated by the measurement of IFT, extraction and expansion behavior. The following understandings were obtained.

- (1) The three ether additives all contain glycol groups, and the molecular weight is relatively low, which leads to their low cloud point pressure and good affinity with CO₂. DEG has a higher solubility in CO₂ under the same temperature and pressure conditions than the other ethers and is more suitable for low formation pressure reservoir conditions.
- (2) The glycol ether additives demonstrate remarkable potential in reducing the IFT and MMP between hexadecane and CO₂. Compared to ethanol additive, DEG exhibits superior performance, with an IFT reduction of 10% higher than that of ethanol at the same mass fraction. Glycol ether additives have high solubility in CO₂ and strong diffusion capability in oil. By adsorbing on the surface of oil droplets, CO₂ and hexadecane are mutually diffused to promote oil and gas miscibility, thereby enhancing oil recovery.
- (3) The conventional swelling factor cannot reflect the extraction and expansion behavior of CO₂ and oil because of the variation of oil volume during the phase equilibrium. A new method to measure the extraction and expansion rates has been established here and can provide precise guidance for oilfield production. The extraction and expansion effects all increase with the increasing pressure. Though the extraction amount of oil is larger than the expansion amount when the pressure is increased to 11.0 MPa, the expansion rate is larger than the extraction rate at the investigated pressure range. The presence of DEG can enhance the extraction rate and expansion rate when the pressure is larger than the cloud point pressure of DEG.
- (4) The glycol ether additives have related physical properties similar to dimethyl ether, low molecular weight and strong diffusion coefficient in crude oil. When injected with CO₂ into the reservoir, the additives can accelerate the interactions between oil and CO₂ by reducing the IFT and enhancing the extraction and expansion behavior, to have great potential in efficiently improving the oil recovery.

CRedit authorship contribution statement

Huan Zhang: Writing – original draft, Resources, Investigation, Formal analysis, Data curation. **Hou-Jian Gong:** Writing – review & editing, Supervision, Project administration, Methodology, Investigation, Funding acquisition, Formal analysis, Conceptualization. **Wei Lv:** Methodology, Formal analysis, Data curation. **Ji-Wei Lv:** Investigation, Formal analysis, Data curation. **Miao-Miao Gao:** Investigation, Data curation. **Shang-Lin Wu:** Investigation, Data curation. **Hai Sun:** Supervision, Project administration, Funding acquisition. **Long Xu:** Supervision, Project administration,

Methodology, Investigation. **Ming-Zhe Dong:** Writing – review & editing, Supervision, Project administration.

Declaration of competing interest

The authors declare that they have no known competing financial interests or personal relationships that could have appeared to influence the work reported in this paper.

Acknowledgements

We gratefully acknowledge financial supports from the National Natural Science Foundation of China (Grant Nos. 42090024, 52174049), and the Natural Science Foundation of Shandong Province of China (No. ZR2019MEE058).

References

- Almobarak, M., Wu, Z., Myers, M.B., et al., 2021. Chemical-assisted minimum miscibility pressure reduction between oil and methane. *J. Pet. Sci. Eng.* 196, 108094. <https://doi.org/10.1016/j.petrol.2020.108094>.
- Andreas, J., Hauser, E., Tucker, W., 2002. Boundary tension by pendant drops 1. *J. Phys. Chem.* 42 (8), 1001–1019. <https://doi.org/10.1021/j100903a002>.
- Beckman, E., 2004. A challenge for green chemistry: designing molecules that readily dissolve in carbon dioxide. *Chem. Commun.* 17, 1885–1888. <https://doi.org/10.1039/B404406C>.
- Choubineh, A., Helalizadeh, A., Wood, D.A., 2019. The impacts of gas impurities on the minimum miscibility pressure of injected CO₂-rich gas–crude oil systems and enhanced oil recovery potential. *Petrol. Sci.* 16, 117–126. <https://doi.org/10.1007/s12182-018-0256-8>.
- Consan, K.A., Smith, R.D., 1990. Observations on the solubility of surfactants and related molecules in carbon dioxide at 50 °C. *J. Supercrit. Fluids* 3 (2), 51–65. [https://doi.org/10.1016/0896-8446\(90\)90008-A](https://doi.org/10.1016/0896-8446(90)90008-A).
- Ding, M., Wang, Y., Wang, W., et al., 2019. Potential to enhance CO₂ flooding in low permeability reservoirs by alcohol and surfactant as co-solvents. *J. Pet. Sci. Eng.* 182, 106305. <https://doi.org/10.1016/j.petrol.2019.106305>.
- Dong, M., Gong, H., Sang, Q., et al., 2022. Review of CO₂-kerogen interaction and its effects on enhanced oil recovery and carbon sequestration in shale oil reservoirs. *Resour. Chem. Mater.* 1 (1), 93–113. <https://doi.org/10.1016/j.recem.2022.01.006>.
- Feng, Q., Xu, S., Xing, X., et al., 2020. Advances and challenges in shale oil development: a critical review. *Adv. Geo-Energy Res.* 4 (4), 406–418. <https://doi.org/10.46690/ager.2020.04.06>.
- Fu, J., Li, S., Niu, X., et al., 2020. Geological characteristics and exploration of shale oil in Chang 7 member of Triassic Yanchang formation, Ordos Basin, NW China. *Petrol. Explor. Dev.* 47 (5), 931–945. [https://doi.org/10.1016/S1876-3804\(20\)60107-0](https://doi.org/10.1016/S1876-3804(20)60107-0).
- Ganjdanesh, R., Rezaeisi, M., Pope, G.A., et al., 2016. Treatment of condensate and water blocks in hydraulic-fractured shale-gas/condensate reservoirs. *SPE J.* 21 (2), 665–674. <https://doi.org/10.2118/175145-PA>.
- Gong, H., Lv, W., Zhang, H., et al., 2024. The influence and mechanism of alkyl block polyethers on the interfacial tension and minimum miscibility pressure of CO₂ and shale oil. *Fuel* 356, 129568. <https://doi.org/10.1016/j.fuel.2023.129568>.
- Han, H., Yuan, S., Li, S., et al., 2015. Dissolving capacity and volume expansion of carbon dioxide in chain *n*-alkanes. *Petrol. Explor. Dev.* 42 (1), 97–103. [https://doi.org/10.1016/S1876-3804\(15\)60011-8](https://doi.org/10.1016/S1876-3804(15)60011-8).
- Janna, F., Le-Hussain, F., 2020. Effectiveness of modified CO₂ injection at improving oil recovery and CO₂ storage—Review and simulations. *Energy Rep.* 6, 1922–1941. <https://doi.org/10.1016/j.egy.2020.07.008>.
- Jia, B., Tsau, J.-S., Barati, R., 2019. A review of the current progress of CO₂ injection EOR and carbon storage in shale oil reservoirs. *Fuel* 236, 404–427. <https://doi.org/10.1016/j.fuel.2018.08.103>.
- Jiang, Z., Zhang, W., Liang, C., et al., 2016. Basic characteristics and evaluation of shale oil reservoirs. *Pet. Res.* 1 (2), 149–163. [https://doi.org/10.1016/S2096-2495\(17\)30039-X](https://doi.org/10.1016/S2096-2495(17)30039-X).
- Kauffman, J.F., 2001. Quadrupolar solvent effects on solvation and reactivity of solutes dissolved in supercritical CO₂. *J. Phys. Chem. A* 105 (14), 3433–3442. <https://doi.org/10.1021/jp004359l>.
- Kazarian, S.G., Vincent, M.F., Bright, F.V., et al., 1996. Specific intermolecular interaction of carbon dioxide with polymers. *J. Am. Chem. Soc.* 118 (7), 1729–1736. <https://doi.org/10.1021/ja950416q>.
- Kharazi, M., Saïen, J., Torabi, M., et al., 2023a. Green nano multicationic ionic liquid based surfactants for enhanced oil recovery: a comparative study on design and applications. *J. Mol. Liq.* 383, 122090. <https://doi.org/10.1016/j.molliq.2023.122090>.
- Kharazi, M., Saïen, J., Torabi, M., et al., 2023b. Molecular design and applications of a nanostructure green Tripodal surface active ionic liquid in enhanced oil recovery: interfacial tension reduction, wettability alteration, and emulsification. *Petrol. Sci.* 20 (6), 3530–3539. <https://doi.org/10.1016/j.petsci.2023.07.010>.

- Kong, S., Feng, G., Liu, Y., et al., 2021. Potential of dimethyl ether as an additive in CO₂ for shale oil recovery. *Fuel* 296, 120643. <https://doi.org/10.1016/j.fuel.2021.120643>.
- Kumar, N., Sampaio, M.A., Ojha, K., et al., 2022. Fundamental aspects, mechanisms and emerging possibilities of CO₂ miscible flooding in enhanced oil recovery: a review. *Fuel* 330, 125633. <https://doi.org/10.1016/j.fuel.2022.125633>.
- Lang, D., Lun, Z., Lv, C., et al., 2021. Nuclear magnetic resonance experimental study of CO₂ injection to enhance shale oil recovery. *Petrol. Explor. Dev.* 48 (3), 702–712. [https://doi.org/10.1016/S1876-3804\(21\)60056-3](https://doi.org/10.1016/S1876-3804(21)60056-3).
- Li, B., Ye, J., Li, Z., 2016. Interphase interaction of CO₂-oil-water system and its influence on interfacial tension under high temperature and pressure. *Acta Pet. Sin.* 37 (10), 1265–1272. <https://doi.org/10.7623/syxb201610006>.
- Li, H., Yang, D., Tontiwachwuthikul, P., 2012. Experimental and theoretical determination of equilibrium interfacial tension for the solvent(s)-CO₂-heavy oil systems. *Energy Fuels* 26 (3), 1776–1786. <https://doi.org/10.1021/ef201860f>.
- Li, H., Zheng, S., Yang, D., 2013. Enhanced swelling effect and viscosity reduction of solvent(s)/CO₂/heavy-oil systems. *SPE J.* 18 (4), 695–707. <https://doi.org/10.2118/150168-PA>.
- Liu, B., Shi, J., Sun, B., et al., 2015. Molecular dynamics simulation on volume swelling of CO₂-alkane system. *Fuel* 143, 194–201. <https://doi.org/10.1016/j.fuel.2014.11.046>.
- Liu, H., Tao, J., Meng, S., et al., 2022. Application and prospects of CO₂ enhanced oil recovery technology in shale oil reservoir. *China Pet. Explore* 27 (1), 127. <https://doi.org/10.3969/j.issn.1672-7703.2022.01.012>.
- Liu, J., Han, B., Li, G., et al., 2001. Solubility of the non-ionic surfactant tetraethylene glycol n-laurel ether in supercritical CO₂ with n-pentanol. *Fluid Phase Equil.* 187, 247–254. [https://doi.org/10.1016/S0378-3812\(01\)00539-8](https://doi.org/10.1016/S0378-3812(01)00539-8).
- Liu, J., Han, B., Wang, Z., et al., 2002a. Solubility of Ls-36 and Ls-45 surfactants in supercritical CO₂ and loading water in the CO₂/water/surfactant systems. *Langmuir* 18 (8), 3086–3089. <https://doi.org/10.1021/la011721u>.
- Liu, J., Han, B., Zhang, J., et al., 2002b. Formation of water-in-CO₂ microemulsions with non-fluorous surfactant Ls-54 and solubilization of biomacromolecules. *Chem. Eur J.* 8 (6), 1356–1360. [https://doi.org/10.1002/1521-3765\(20020315\)8:6](https://doi.org/10.1002/1521-3765(20020315)8:6).
- Luo, H., Zhang, Y., Fan, W., et al., 2018. Effects of the non-ionic surfactant (C₆PO₂) on the interfacial tension behavior between CO₂ and crude oil. *Energy Fuels* 32 (6), 6708–6712. <https://doi.org/10.1021/acs.energyfuels.8b01082>.
- Lv, W., Gong, H., Dong, M., et al., 2024. Potential of nonionic polyether surfactant-assisted CO₂ huff-n-puff for enhanced oil recovery and CO₂ storage in ultra-low permeability unconventional reservoirs. *Fuel* 359, 130474. <https://doi.org/10.1016/j.fuel.2023.130474>.
- Lv, W., Gong, H., Li, Y., et al., 2020. Dissolution behaviors of alkyl block polyethers in CO₂: experimental measurements and molecular dynamics simulations. *Chem. Eng. Sci.* 228, 115953. <https://doi.org/10.1016/j.ces.2020.115953>.
- Moradi, B., Awang, M., Bashir, A., et al., 2014. Effects of alcohols on interfacial tension between carbon dioxide and crude oil at elevated pressures and temperature. *J. Pet. Sci. Eng.* 121, 103–109. <https://doi.org/10.1016/j.petrol.2014.06.017>.
- Ozowe, W., Zheng, S., Sharma, M., 2020. Selection of hydrocarbon gas for huff-n-puff IOR in shale oil reservoirs. *J. Pet. Sci. Eng.* 195, 107683. <https://doi.org/10.1016/j.petrol.2020.107683>.
- Ryoo, W., Webber, S.E., Johnston, K.P., 2003. Water-in-carbon dioxide microemulsions with methylated branched hydrocarbon surfactants. *Ind. Eng. Chem. Res.* 42 (25), 6348–6358. <https://doi.org/10.1021/jie0300427>.
- Saien, J., Kharazi, M., Shokri, B., et al., 2023. A comparative study on the design and application of new nano benzimidazolium gemini ionic liquids for curing interfacial properties of the crude oil–water system. *RSC Adv.* 13 (23), 15747–15761. <https://doi.org/10.1039/D3RA01783D>.
- Saira, S., Yin, H., Le-Hussain, F., 2020. Using alcohol-treated CO₂ to reduce miscibility pressure during CO₂ injection. In: Proceedings of SPE Asia Pacific Oil and Gas Conference and Exhibition. <https://doi.org/10.2118/202341-MS>.
- Saira, S., Ajoma, E., Le-Hussain, F., 2021. A laboratory investigation of the effect of ethanol-treated carbon dioxide injection on oil recovery and carbon dioxide storage. *SPE J.* 26 (5), 3119–3135. <https://doi.org/10.2118/205503-PA>.
- Sayed, M.A., Al-Muntasheri, G.A., 2014. Liquid bank removal in production wells drilled in gas-condensate reservoirs: a critical review. In: Proceedings of SPE International Conference and Exhibition on Formation Damage Control. <https://doi.org/10.2118/168153-MS>.
- Sheng, J.J., 2015. Enhanced oil recovery in shale reservoirs by gas injection. *J. Nat. Gas Sci. Eng.* 22, 252–259. <https://doi.org/10.1016/j.jngse.2014.12.002>.
- Song, Y., Song, Z., Zhang, Y., et al., 2022. Pore scale performance evaluation and impact factors in nitrogen huff-n-puff EOR for tight oil. *Petrol. Sci.* 19 (6), 2932–2940. <https://doi.org/10.1016/j.petsci.2022.05.012>.
- Taheri-Shakib, J., Kantzas, A., 2021. A comprehensive review of microwave application on the oil shale: prospects for shale oil production. *Fuel* 305, 121519. <https://doi.org/10.1016/j.fuel.2021.121519>.
- Tang, W., Sheng, J.J., Jiang, T., 2023. Further discussion of CO₂ huff-n-puff mechanisms in tight oil reservoirs based on NMR monitored fluids spatial distributions. *Petrol. Sci.* 20 (1), 350–361. <https://doi.org/10.1016/j.petsci.2022.08.014>.
- Tsukahara, T., Kayaki, Y., Ikariya, T., et al., 2004. ¹³C NMR spectroscopic evaluation of the affinity of carbonyl compounds for carbon dioxide under supercritical conditions. *Angew. Chem. Int. Ed.* 43 (28), 3719–3722. <https://doi.org/10.1002/anie.200454190>.
- Wang, H., Luo, M., Lun, Z., et al., 2018. Determination and comparison of interfacial interactions between CO₂, crude oil, and brine at reservoir conditions. *Energy Fuels* 32 (8), 8187–8192. <https://doi.org/10.1021/acs.energyfuels.8b01446>.
- Wei, B., Gao, H., Pu, W., et al., 2017. Interactions and phase behaviors between oleic phase and CO₂ from swelling to miscibility in CO₂-based enhanced oil recovery (EOR) process: a comprehensive visualization study. *J. Mol. Liq.* 232, 277–284. <https://doi.org/10.1016/j.molliq.2017.02.090>.
- Xu, Y., Lun, Z., Pan, Z., et al., 2022. Occurrence space and state of shale oil: a review. *J. Petrol. Sci. Eng.* 211, 110183. <https://doi.org/10.1016/j.petrol.2022.110183>.
- Yang, L., Jin, Z., 2019. Global shale oil development and prospects. *China Pet. Explore* 24 (5), 553. <https://doi.org/10.3969/j.issn.1672-7703.2019.05.002>.
- Yang, W., Chang, Y., Cheng, J., et al., 2021. Effects of pore structures on seepage and dispersion characteristics during CO₂ miscible displacements in unconsolidated cores. *Energy Fuels* 35 (21), 17791–17809. <https://doi.org/10.1021/acs.energyfuels.1c02299>.
- Yu, W., Lashgari, H.R., Wu, K., et al., 2015. CO₂ injection for enhanced oil recovery in Bakken tight oil reservoirs. *Fuel* 159, 354–363. <https://doi.org/10.1016/j.fuel.2015.06.092>.
- Zhang, C., Xi, L., Wu, P., et al., 2020. A novel system for reducing CO₂-crude oil minimum miscibility pressure with CO₂-soluble surfactants. *Fuel* 281, 118690. <https://doi.org/10.1016/j.fuel.2020.118690>.
- Zhang, K., Jia, N., Zeng, F., et al., 2019. A review of experimental methods for determining the oil-gas minimum miscibility pressures. *J. Pet. Sci. Eng.* 183, 106366. <https://doi.org/10.1016/j.petrol.2019.106366>.
- Zhang, K., Liu, L., Huang, G., 2020. Nanoconfined water effect on CO₂ utilization and geological storage. *Geophys. Res. Lett.* 47 (15), e2020GL087999. <https://doi.org/10.1029/2020GL087999>.
- Zhang, N., Wei, M., Bai, B., 2018. Statistical and analytical review of worldwide CO₂ immiscible field applications. *Fuel* 220, 89–100. <https://doi.org/10.1016/j.fuel.2018.01.140>.
- Zhu, T., Gong, H., Dong, M., et al., 2018. Phase equilibrium of PVAc+CO₂ binary systems and PVAc+CO₂+ethanol ternary systems. *Fluid Phase Equil.* 458, 264–271. <https://doi.org/10.1016/j.fluid.2017.11.029>.
- Zou, C., Zhu, R., Bai, B., et al., 2015. Significance, geologic characteristics, resource potential and future challenges of tight oil and shale oil. *Bull. China Soc. Mineral Petrol. Geochem.* 34 (1), 3–17. <https://doi.org/10.3969/j.issn.1007-2802.2015.01.001>.